MAGNETIC BEARINGS AS AN IMPELLER FORCE MEASUREMENT TECHNIQUE

by

Adiel Guinzburg

Staff Researcher

and

Frederic W. Buse

Senior Engineering Consultant

Ingersoll-Dresser Pump Company

Phillipsburg, New Jersey

Adiel Guinzburg is a Staff Researcher at Ingersoll-Dresser Pump Company. Prior to joining Ingersoll-Dresser Pump Company, she was a Research Scientist at the Institut de Machines Hydrauliques et de Mécaniques des Fluides at the Ecole Polytechnique Fédérale de Lausanne, Switzerland. She received a B.Sc degree in Aeronautical Engineering (1985) from the University of the Witwatersrand, an M.S. degree (1986) and a Ph.D. degree (1991) from the California Institute of Technology. Dr. Guinzburg is a member of ASME and AIAA and is the author of several technical papers.

Frederic W. Buse is a Senior Engineering Consultant at Ingersoll-Dresser Pump Company, where he has been employed for 36 years. He is a graduate of New York Maritime College, with a B.S. degree (Marine Engineering). He is a member of the Hydraulic Institute and of ANSI Committees B73.1 for horizontal centrifugal pumps and B73.2 for vertical chemical pumps.

He has contributed to Marks' Standard Handbook for Mechanical Engineers, *the* Pump Handbook, *and* Pump Application and Design. *He has written numerous articles for periodicals and has received 17 U.S. Patents on centrifugal and reciprocating pumps. He has contributed to API on writing the specifications for reciprocating pumps (API 674) and has also contributed to the writing of the ASME test code on centrifugal pumps.*

Mr. Buse represents the United States for writing the ISO centrifugal pump standards. He is chairman of the Hydraulic Institute Test Standards Committee, and Sealless Pump Committee. He has also been author and co-author of several papers and tutorials for the International Pump Users Symposiums.

ABSTRACT

The technique of measuring steady loads on centrifugal pump impellers via magnetic bearings is demonstrated and shown to be a reliable way of clarifying loads, which have been traditionally difficult to determine both analytically and experimentally. Among the most challenging geometries in this respect is the semiopen impeller in an end-suction single volute pump. Because of the uneven distribution of the pressure on the shroud of a semiopen impeller, axial and radial loads are created. In addition to the classical axial and radial loads, it is recognized that a hydraulic couple is also generated with semiopen impellers. The hydraulic couple is not discussed. In the past, experimental evaluation of the hydraulic forces and moments on impellers has been accomplished through techniques such as strain measurements and static pressures at taps in the walls adjacent to the impeller. The present experimental results are obtained using the magnetic bearing test rig that was designed to measure the forces and moments that result from the hydrodynamic interactions in a centrifugal pump under various operating conditions. The comparison is presented between the results for the single stage pump obtained by the traditional methods and those derived from magnetic bearing reactions. The results are given for the full range of flowrates from shutoff to runout and a Reynolds number effect is also examined for semiopen impellers. The information obtained will be used to design new industrial pumps.

INTRODUCTION

Turbomachinery designers have focused on the search for new concepts to meet the reliability, efficiency, safety standards and stringent cost effectiveness that must be met today. When designing turbomachinery, it is important to be able to predict the fluid-induced forces to determine bearing life and shaft deflections. Empirical methods for evaluating the loads on impellers have led to predictions that are orders of magnitude apart. Thus, an experimental rig was designed to determine these loads.

The impeller and the volute casing are designed to provide a circumferentially uniform discharge flow pattern at design conditions that coincide with the best efficiency point (bep). However at off-design conditions, the volute flow pattern is no longer uniform; when the flowrate changes, the volute conditions become asymmetric. This results in a net radial force due to the asymmetric pressure discharge condition. Note that even at the design flowrate, the discharge conditions could be asymmetric if the impeller is displaced from the design center by shaft deflection or bearing wear. Hydrodynamic interactions in centrifugal pumps have typically focused on these radial and axial forces.

There are two sources that contribute to the radial hydrodynamic forces on the impeller. One is due to the asymmetric distributions around the impeller and the other is caused by the asymmetric momentum fluxes at the impeller suction and discharge. The first contribution can be evaluated by integrating the asymmetric pressure distribution around the suction and discharge of the impeller. The momentum fluxes result in negligible contribution to the net force on single stage end suction pumps below a specific speed of 3000.

Because of the uneven distribution of the pressure on the shroud in volute end suction pumps with a semiopen impeller, there is an additional component that manifests itself as a moment [1]. This can lead to increased shaft deflection, shaft stress and decreased bearing life, and frequent shutdowns to replace components. This study investigates the forces but does not discuss the moments that result from the hydrodynamic interactions in a centrifugal pump with a semiopen impeller.

BACKGROUND

Fluid-induced rotordynamic forces on impellers in turbomachines are now well recognized. The forces are defined by expressing the instantaneous forces, Fx (t), Fy(t) and Fz(t) (figure 1) acting on the impeller in the linear form:

$$\begin{pmatrix} F_x \\ F_y \\ F_z \\ m_x \\ m_y \end{pmatrix} = \begin{pmatrix} F_{ox} \\ F_{oy} \\ F_{oz} \\ m_{ox} \\ m_{oy} \end{pmatrix} + [A] \cdot \begin{pmatrix} x(t) \\ y(t) \\ z(t) \\ \theta(t) \\ \theta(t) \end{pmatrix} \quad (1)$$

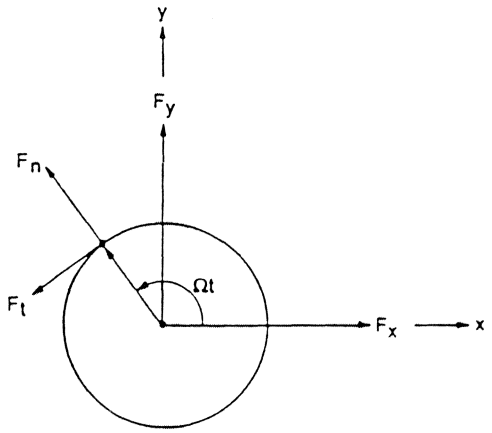

Figure 1. Definition of the Fluid Forces on a Pump.

The first term on the right hand side represents the steady, time-averaged forces, in a stationary frame and [A] is the rotordynamic matrix where x(t), y(t), z(t) are the shaft displacements from the mean position. The steady radial forces, F_{ox}, F_{oy}, F_{oz}, or hydraulic loads result from asymmetries in the flow and have been measured by several authors [2, 3, 4, 5, 6]. The rotordynamic matrix, [A], will, in general, be a function of the mean flow conditions and pump geometry along with of the whirl motion. Rotordynamic forces imposed on a centrifugal impeller by the fluid flow were first measured by Domm and Hergt [4], Hergt and Krieger [7], Chamieh, et al. [5], Jery, et al. [8], and Ohashi, et al. [9].

For the present discussion, the emphasis will be on the steady forces. There are several empirical values that are used by pump designers to estimate these forces. These approximations do not include differences between an open impeller *vs* a closed impeller for the radial load, or the influence of scallops in the impeller disk (Figure 2) on the radial load, axial load, and moment. Experimental results of the hydraulic loads for semiopen impellers with scallops in the shroud as a function of impeller diameter and back shroud clearance variation have not been presented up to now. The hydraulic loads are obtained from the magnetic bearings, including the clearance effect covered in this study. Radial thrust factors are compared with the empirical results.

Radial Force

Several empirical methods for estimating the radial forces on closed impellers have been developed and have been successfully used for shaft deflection, shaft sizing, and bearing selection. The magnitude and location of the radial force acting on the impeller depends on the operating point relative to the best efficiency point (bep) and specific speed. Since single and double volutes of spiral form are typically designed for uniform velocity around the volute or casing at the design capacity, the radial force is usually a minimum at best efficiency and a maximum at shutoff. This flow cannot be maintained at off design flowrates. Therefore, away from the best efficiency point, the nonuniform pressure distribution results in a radial force acting on the impeller:

$$F = \frac{K.\gamma.H.D_2.b}{2.31} \quad (2)$$

where

b is the overall width of the impeller including shrouds, in

D_2 is the impeller diameter, in

F is the radial force, lbf

H is the developed head, ft

K is an empirical constant

γ is the specific gravity

The earliest correlation for the radial load on a single-volute centrifugal pump was by Stepanoff [10] who estimated the empirical constant as a function of the capacity:

$$K = 0.36\left(1 - \left(\frac{Q}{Q_n}\right)^2\right) \quad (3)$$

where

Q is the flowrate where the force is evaluated.

Q_n is the flowrate at the best efficiency point.

The technique used for determining the forces was by measuring the shaft deflection and calibrating with weights. Subsequently, K values for a single spiral volute were determined experimentally by Agostinelli, et al. [3], as a function of flow and specific speed. This observation was important as the specific speed characterizes the impeller geometry of both the impeller and the volute casing. Presently, the Hydraulic Institute technical specification TS001-C [11] is the standard for the calculation of radial thrust for a volute pump.

Biheller [12] also presented a semiempirical relation for the radial load in a slightly different form. In this relation, the influence of the cutwater clearance on the force is accounted for. The equation simplifies for a fully volute pump as folllows:

$$F = 4.76 \times 10^{-5}\left(U_2^2 A_i \rho \times 10^{(-1.13 A_i/A_\infty)}\right) \sqrt{1 + \left(\frac{Q}{Q_n}\right)^2 - 2\left(\frac{Q}{Q_n}\right)\cos\left[-\frac{\pi}{2} + \left(\frac{\pi}{2}\right)\frac{Q}{Q_n}\right]} \quad (4)$$

where

A_i is the impeller projected area, (diameter x impeller overall width), in^2.

A_t is the collector cross-sectional area at the tongue, in^2.

$A\infty$ (is the collector cross-sectional area at the throat, in^2.

u_2 is the tangential velocity of the impeller, ft/sec.

ρ is the fluid density, lbm/ft^3.

Axial Force

In a centrifugal pump, the different pressure distributions between the front and rear shrouds generally result in an axial force towards the suction. The classic equation for the axial force on an enclosed impeller is a function of the developed head and specific speed. The Hydraulic Institute Standards describe the axial force as the difference between the axial force generated on the front shroud and the axial force on the back shroud on an enclosed impeller:

$$F_z = \frac{\gamma.H}{2.31} \cdot [K_B A_B - K_F A_F]$$

$$A_B = \frac{\pi}{4} (D_2^2 - D_h^2)$$

$$A_F = \frac{\pi}{4} (D_2^2 - D_R^2)$$

$$K_B = \frac{K_2 + K_h}{2}$$

$$K_F = \frac{K_2 + K_R}{2}$$

hence,

$$F_z = \frac{\gamma.H}{2.31} \cdot \left[\left(\frac{K_2 + K_h}{2} \right) (A_2 - A_h) - \left(\frac{K_2 + K_R}{2} \right) (A_2 - A_R) \right] \quad (5)$$

where

A_B is the area exposed to pressure on the back shroud, in^2.

A_F is the area exposed to pressure on the front shroud, in^2.

A_h is the shaft area, in^2.

A_R is the front ring area, in^2.

A_2 is the impeller diameter area.

D_h is the hub diameter, in.

D_R is the front ring diameter, in.

D_2 is the impeller diameter, in.

H is the developed head, ft.

K_B is an empirical constant that represents the percent of developed head on the back shroud.

K_F is an empirical constant that represents the percent of developed head on the front shroud.

K_h is an empirical constant that represents the percent of developed head at the hub diameter.

K_R is an empirical constant that represents the percent of developed head at the ring diameter.

K_2 is an empirical constant that represents the percent of developed head at the impeller diameter

γ is the specific gravity.

The Hydraulic Institute Standards tabulate values for the empirical factor K for enclosed impellers, as a function of the ratio of the diameter where K is being evaluated to the exit diameter of the impeller. The distribution is a strong function of specific speed, and it is also influenced by the ring clearance. Impeller designs employ back vanes, back rings, balance holes or scalloping as a means to reduce the axial thrust [13]. The effect of these configurations on the force is demonstrated in Table 1.

Table 1. Empirical Determination of Axial Force.

Configuration	K_h
Plain shroud	0.4
Back vanes	0.1 to 0.25
Back ribs with balance holes	0.1

The calculation of the axial force on a semiopen impeller is similar to that shown for an enclosed impeller, except that the K_h factor for the hub can vary greatly depending on the design of the impeller. Some of these variations are as follows:

- plain shrouds
- shrouds with scallops
- shrouds with pumpout vanes
- shrouds with pumpout slots
- shrouds with balance holes
- shrouds with pump out vanes and balance holes
- combinations of the above with scallops

The changes of the K_h factor as a result of all these configurations is not discussed here. However, future tests are planned to explore these effects.

EXPERIMENTAL FACILITY

In the past, experimental evaluation of the hydraulic forces on impellers has been accomplished via techniques such as strain measurements and static pressures at taps in the walls adjacent to the impeller. Previous test rigs (Chamieh, et al. [5], Bolleter, et al. [4], and Ohashi and Shoji [15]) required slip ring assemblies to transport the force signal from the rotating member to the acquisition system. The advantage of an active magnetic bearing concept is that the fluid-structure interaction problems in pumps, compressors, turbines and other machines can be investigated through noncontact with the rotor [16, 17]. The present experimental results are obtained using such a magnetic bearing test rig. This rig contains three magnetic bearings, two of that sense radial forces and one that senses axial thrust (Figures 3 and 4).

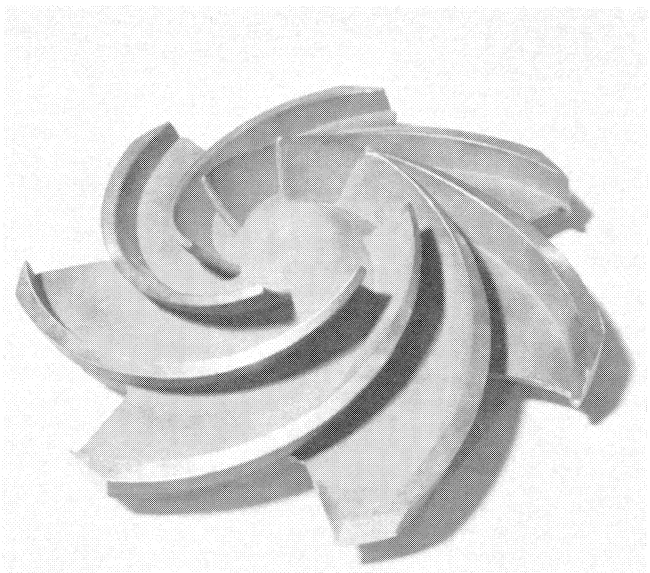

Figure 2. Test Impeller. Note scallops in impeller back shroud.

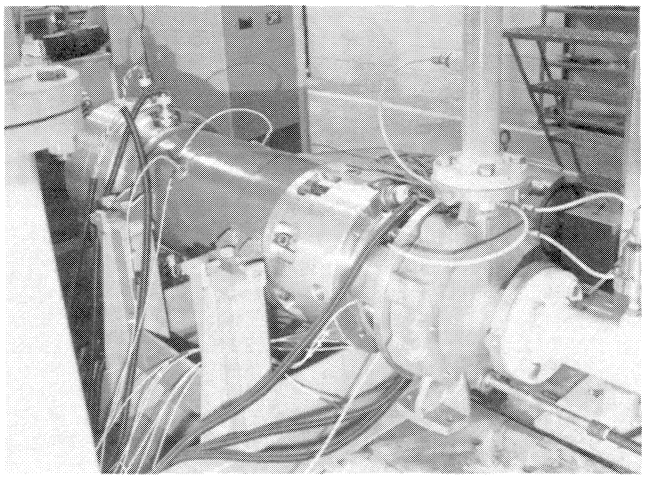

Figure 3. Magnetic Bearing Test Rig with a Centrifugal Pump in the Foreground.

The impeller (Figure 2) is mounted on the main shaft of the rig (Figure 5). The rotor is suspended in a magnetic field generated by magnets mounted around the rotor. A control circuit (Figure 6) is used to alter the current in the coils, and, hence, the magnetic field in response to the shaft positions that are sensed by the proximity probes. The bearing force is directly implied from the magnetic bearing current and rotor position. This allows identification of the radial impeller forces, axial impeller force and impeller moments. Thus, the magnetic bearings serve two functions: to keep the rotor centered in the stator and to act as force sensors.

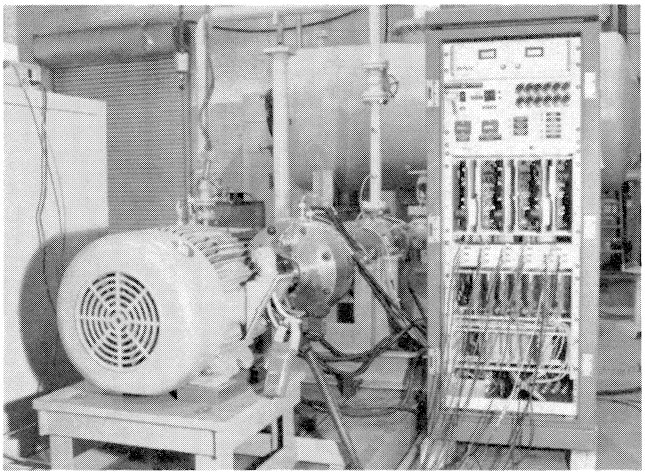

Figure 4. Control Unit for the Magnetic Bearing Test Rig.

Each radial bearing has two displacement sensors arranged 90 degrees apart. One axial displacement sensor is used for the control of the axial bearing. In addition four axial sensors, spaced 90 degrees apart are located on a disk behind the impeller. These latter probes give a qualitative indication of the hydraulic moment and verify the calculation of the impeller moment implied from the forces at the magnetic bearings. A shaft encoder provides a once per revolution signal. A multiplier increases the number of pulses per revolution and is the trigger pulse for data acquisition. This limits the fluctuations associated with small changes in shaft speed. The motor is equipped with an

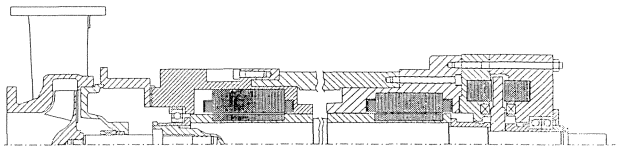

Figure 5. Schematic of the Magnetic Bearing Test Rig. Note the locations of the two radial and single double-acting axial magnetic bearings.

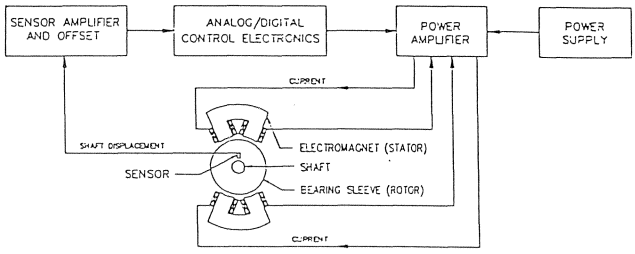

Figure 6. Magnetic Bearing Control Scheme.

adjustable speed control, so that tests at diferent rotational speeds can be conducted, and the effect of Reynolds number on the hydraulic forces can be evaluated. In addition to the current and displacement signals being sampled, flowrate, suction pressure, discharge pressure, and torque measurements are taken. Pressure taps are provided on the casing for determining the hydraulic forces resulting from the pressure distribution for comparison with the loads obtained with the magnetic bearings.

Impeller Force Calculation

The bearing reaction is calculated from the measured currents and displacement. The force equation for a single axis of a magnetic bearing is a nonlinear function. The magnitude of the force exerted by the electromagnets is proportional to the square of the current in the coils and inversely proportional to the square of the air gap:

$$F = \mu_o c_g A_g N^2 \left[\left(\frac{i_A}{c_A} \right)^2 - \left(\frac{i_B}{c_B} \right)^2 \right] \qquad (6)$$

where

A_g is the cross sectional area of the flux path, m^2.

c_g is a geometry correction factor.

c_A, c_B represent the top and bottom effective radial clearances on each bearing axis respectively, m.

i_A and i_B represent the current in the top and bottom magnet pair, (A).

N is the number of turns per magnet.

μ_0 is the permeability of the free space between the rotor and stator, ($4\pi \times 10$ -7 H/m)

Active magnetic bearings are nonlinear due to the nonlinearities of electromagnetic fields. Also, there are force coupling effects among the various axes. The nonlinear nature results in an increase in the modelling complexity and control of the bearings.

Before the forces at the impeller can be determined, a bearing bias force correction and offset calibration must be made. The procedure involves applying a known force to the bearing axis such as the component of weight supported by that axis. This is done by levitating the shaft at the start of each experiment to

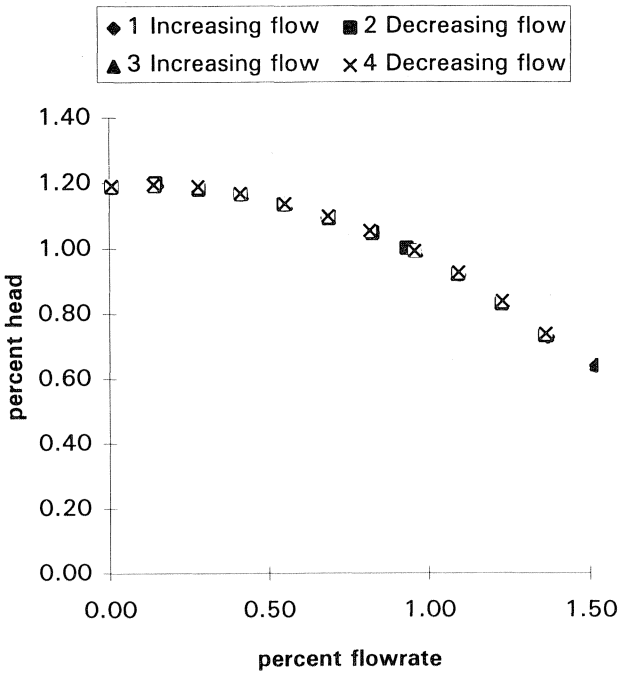

Figure 7. Pump Characteristics of the Test Impeller.

determine the actual top and bottom effective clearances, for each bearing axis, c_A and c_B. The magnetic bearing actuators and sensors are not collocated axially; however, this position error is accounted for in the analysis procedure. Using this result, along with as the measured currents and displacements, the bearing reaction force is calculated as a result of the applied forces and moments on the impeller. The radial impeller forces are determined by summation of forces and moments obtained at the bearings. The impeller axial force is assumed to be that measured at the thrust bearing. The impeller moments are determined by summation of moments at the impeller centerline.

Calibration

The bearings have a radial force capacity of 6 672 N (1500 lbf) each and an axial force capacity of 35 584 N (8000 lbf) in either direction. A loading fixture has been designed and is used to determine the relationships between the bearing currents and impeller forces via static calibration. Thus, the reactions of the loads at the bearings are calculated and compared to the known applied loads. The loading procedure includes loading the shaft with a moment arm. A hysteresis curve was also generated as the loads were decreased and found not to be significant with a calibration error of five to ten percent. The calibration is independent of operating speeds.

In order to limit the electrical noise on the current signals, a simple R-C filter of 600 Hz was installed on the controller card. This filter cleaned up some of the noise on the currents, and reduced the scatter on the force data. The signal to noise ratio was improved by amplifying the power amplifier current signals. The data acquisition system (DA) introduced an oscillation that was eliminated by bypassing the DA input port with a 0.01 microfarad capacitor. The combined effects of filtering, bypassing, and amplification provided consistent results.

RESULTS

The objective of this test rig (Figure 3) is to determine the relationship of hydraulic forces of different impeller geometries at various operating conditions. This magnetic bearing test rig is designed to evaluate the forces and moments for a wide range of commercial pumps. The initial test utilizing this rig is of a single stage end suction volute process pump with a semiopen impeller with back vanes. The results will be used to design new industrial pumps. The pump characteristics for this centrifugal pump with a single spiral volute are as shown in Table 2.

Table 2. The Pump Characteristics (Figure 2).

head at 3550 RPM	120 m	393 ft
flow at 3550 RPM	91m³/h	400 gpm
speed range	900-3550 RPM	900-3550 rpm
test speed	900-1780 RPM	900-1780 rpm

The comparison between the results derived from magnetic bearing reactions for this pump is made with other traditional methods used for enclosed impellers in Table 3. The results are presented nondimensionalized by the impeller OD dynamic head and the area where the force is acting:

$$K_R = \frac{F_R}{\frac{1}{2}\rho.u^2bD} \tag{7}$$

and

$$K_Z = \frac{F_Z}{\frac{1}{2}\rho.u^2\pi.R^2} \tag{8}$$

where

b is the overall width at the impeller discharge, including shrouds (m).

D is the impeller diameter, (m).

F_R is the radial force, (N).

F_Z is the axial force, (N).

R is the radius at the impeller discharge,(m).

$u = \omega R$ is the impeller peripheral velocity, (m/s).

ρ is the fluid density, (kg/m3).

ω is the rotor speed, (rad/s).

Table 3. Predicted and Measured Nondimensional Radial Forces.

	(a) dynamic head			(b) shut-off head
Method	0% flow	50% flow	100% flow	0% flow
Stepanoff	0.455	0.355	0	0.36
Agostinelli	0.157	0.069	0.009	0.124
Biheller	0.301	0.222	0	0.239
Present data	0.3	0.15	0.05	0.237

In Figures 8, 9, 10, 11, 12, and 13, the results are given for the full range of flowrates from shutoff to runout. The variation of the radial forces is shown to be a strong function of flow. As shown by other investigations, the radial force is a maximum at shutoff and is not a minimum at bep. The minimum can be seen to lie between 70 percent and 90 percent of bep. Note that the shape of the radial load versus flow is similar (V-shape) to that for a closed impeller. On the other hand, the shape of the axial

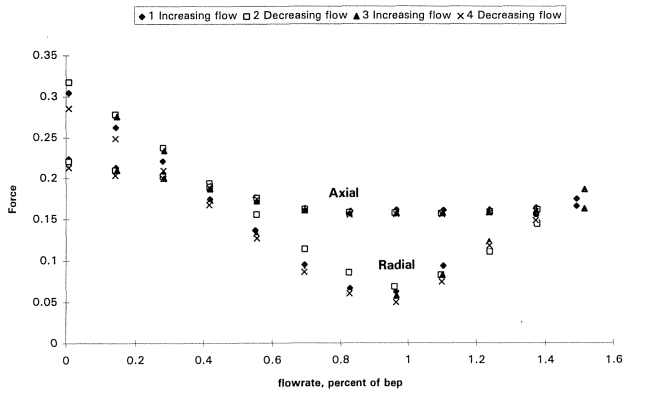

Figure 8. Nondimensionalized Radial and Axial Forces Measured with the Magnetic Test Rig at 1780 RPM. Series 1 and 3 were measured for decreasing flow; series 2 and 4 were for increasing flow. The back clearance is 0.762 mm (0.030 in) and the front clearance is 0.3302 mm (0.013in).

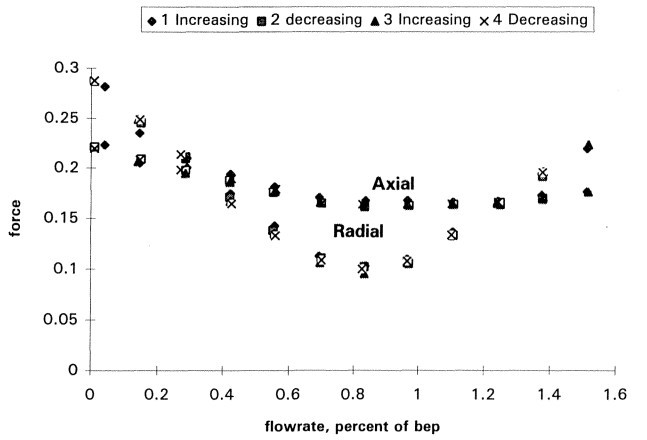

Figure 9. Nondimensionalized Radial and Axial Forces Measured with the Magnetic Test Rig at 1180 RPM. Series 1 and 3 were measured for decreasing flow; series 2 and 4 were for increasing flow. The back clearance is 0.762 mm (0.030 in) and the front clearance is 0.3302 mm (0.013in).

thrust versus flow does not follow bep flow as is usually shown for closed impellers.

In Figure 8, the test operating speed is 1780 rpm and the back clearance between the back vanes and the casing is 0.76 mm (0.030 in). The same configuration is shown at an operating speed of 1180 rpm in Figure 9. The back clearance is increased to 1.27 mm (0.050 in) in Figures 10 and 11. A larger back clearance diminishes the ability of the radial vanes on the back of the impeller to reduce the pressure behind the impeller. Thus, the axial force in the direction of suction must increase when the back clearance is increased. Indeed, this can be seen to occur when comparing Figures 9 and 11.

The traditional equation to predict the axial force for an enclosed impeller produces a curve parallel to the pump performance curve. In the case of these semiopen impellers, it can be seen that the axial load is influenced by the pressure distribution around the volute, as is the radial load. It should be noted that the axial load follows the same trend as the radial load and the minimum load value is at the same flow point as the radial load minimum. The prediction of the axial load for semiopen impellers by the empirical relation of Stepanoff [10] yields a nondi-

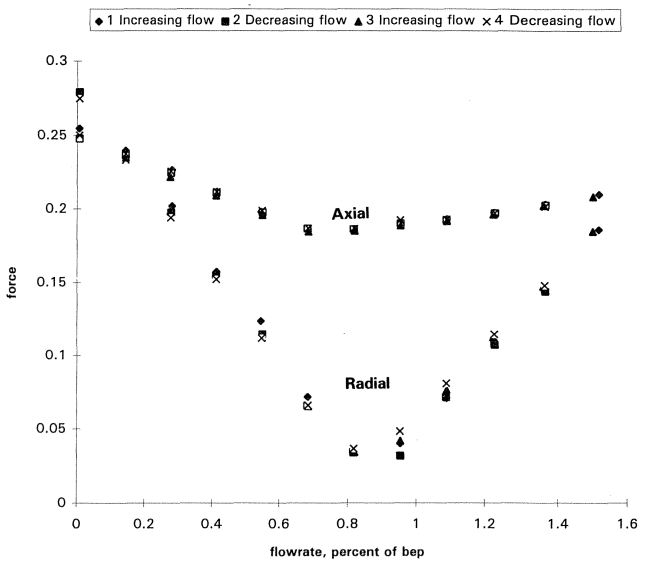

Figure 10. Nondimensionalized Radial and Axial Forces Measured with the Magnetic Test Rig at 1780 RPM. Series 1 and 3 were measured for decreasing flow; series 2 and 4 were for increasing flow. The back clearance is 1.27 mm (0.050 in) and the front clearance is 0.3302 mm (0.013in).

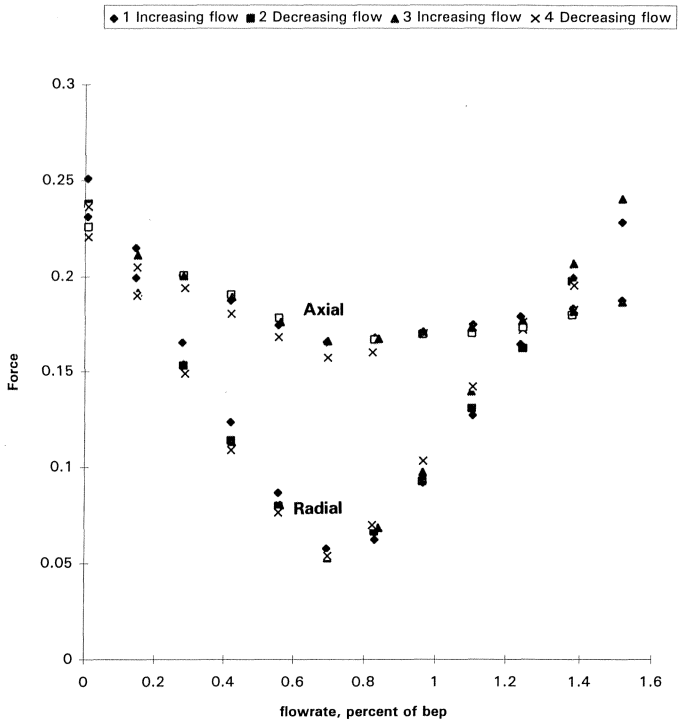

Figure 11. Nondimensionalized Radial and Axial Forces Measured with the Magnetic Test Rig at 1180 RPM. Series 1 and 3 were measured for decreasing flow; series 2 and 4 were for increasing flow. The back clearance is 1.27 mm (0.050 in) and the front clearance is 0.3302 mm (0.013in).

mensionalized value of 0.336 compared with the presently obtained results of 0.25. This discrepancy is not too surprising as the scalloped region is not accounted for in the Stepanoff approach. The method of the Hydraulic Institute for an enclosed impeller, given by Equation (5) predicts a value of 0.18.

An overlay is shown in Figure 12 of the results of Figures 8 and 9 at 0.762 mm (0.030 in) back clearance. An overlay is shown in Figure 13 of the results of Figures 10 and 11 at 1.27 mm (0.050 in) back clearance. No appreciable Reynolds number effect can be observed with the smaller back clearance within the

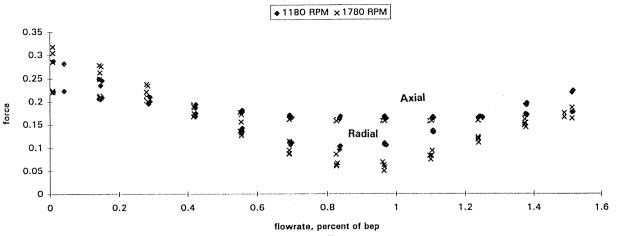

Figure 12. Nondimensionalized Radial and Axial Forces Measured with the Magnetic Test Rig at 1180 RPM and 1780 RPM. The back clearance is 0.762 mm (0.030 in) and the front clearance is 0.3302 mm (0.013in).

range of the experimental data. The main conclusion to draw from this is that the radial and axial loads do scale as the square of the speed. Although at the larger back clearance, Reynolds number effects can be seen to come into play (Figure 13).

The radial forces nondimensionalized are presented in two ways in Table 3. The first (a) nondimensionalizes the forces by the dynamic head, as described in Equation (7). For comparison, the loads at shutoff are also nondimensionalized by the shutoff head (b).

The shutoff head is typically 20 percent to 30 percent larger than the impeller OD dynamic head and will thus result in a lower dimensionless value. At shut-off, the Agostinelli, et al. [3], empirical method under-predicts the radial load, whereas the Stepanoff [10] method gives a high value. This is because the Stepanoff factor does not account for specific speed or geometry changes. This has been an observation among pump designers for enclosed impellers. The present data are for an open impeller with scallops. The typical gap from a shroud to the casing or cover wall with an enclosed impeller is 9.652 mm (0.38 in), where for a semiopen impeller, the clearance is 0.254 to 0.508 mm (0.01 to 0.02 in) on the front and 0.762 to 2.032 mm (0.03 to 0.08 in) on the back. The 9.652 mm gap of the enclosed impeller will allow some equalization of the pressure variation around the volute, resulting in a lower factor than for a semiopen impeller.

CONCLUSIONS

The emphasis of this study is to investigate the steady forces acting on the rotor and casing due to fluid flow in a centrifugal pump with the new concept of measuring magnetic bearing reactions. Herein, the comparison between the results for a single stage pump obtained by several empirical methods and those derived from magnetic bearing reactions are presented. Empirical relationships that do not account for the impeller-casing geometry, specific speed, or shroud configuration do not accurately predict the impeller forces. The main conclusion to draw from the test results is that the radial and axial loads do scale as the square of the speed. An important observation is that the radial thrust factors of semiopen impellers are greater than for an equivalent enclosed impeller. Preliminary results show the axial force to increase with back clearance, while the variation of the radial force is not yet conclusive. Further tests are planned at different operating points, impeller diameter cuts, and different front and back clearances. It is also planned to

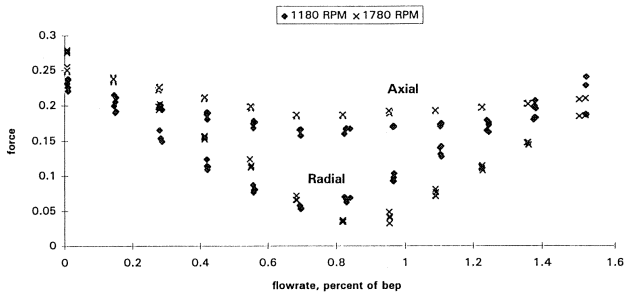

Figure 13. Nondimensionalized Radial and Axial Forces Measured with the Magnetic Test Rig at 1180 RPM and 1780 RPM. The back clearance is 1.27 mm (0.050 in) and the front clearance is 0.3302 mm (0.013in).

evaluate the forces for a series of similar pumps for a range of specific speeds. In the future, the same magnetic bearings will be used to evaluate steady and fluctuating loads in larger, multi-stage pumps. This testing shows that a magnetic bearing test rig will obtain accurate results for evaluating hydraulic forces.

ACKNOWLEDGMENTS

The authors would like to thank the management of Ingersoll-Dresser Pump Company for granting permission for publication, and in particular Ian Massey and Paul Cooper. We would also like to thank Joe Imlach of Imlach Consulting Engineering and those from Kingsbury, Inc. who participated in this project.

REFERENCES

1. Buse, F. W., "The Hydraulic Couple," Ingersoll-Rand Company, internal publication (July 1979).
2. Iversen, H. W., Rolling, R. E., and Carlson, J. J., "Volute Pressure Distribution, Radial Force on the Impeller, and Volute Mixing Losses of a Radial Flow Centrifugal Pump," Journal of Engineering for Power, *82*, pp. 136-144 (1960).
3. Agostinelli, A., Nobles, D., and Mockrige, C.R., "An Experimental Determination of Radial Thrust in Centrifugal Pumps," Journal of Engineering for Power, *82*, pp. 120-126 1960).
4. Domm, U. and Hergt, P., "Radial Forces on Impeller of Volute Casing Pumps," Flow *Research on Blading*, L.S. Dzung, Editor. The Netherlands: Elsevier Publishing Co., pp. 305-321 (1970).
5. Chamieh, D. S., Acosta, A. J., Brennen, C. E., and Caughey, T. K., "Experimental Measurements of Hydrodynamic Radial Forces and Stiffness Matrices for a Centrifugal Pump Impeller," ASME Journal of Fluids Engineering, *107*, (3), pp. 307-315 (1985).
6. Adkins, D. R. and Brennen, C. E., "Analyses of Hydrodynamic Radial Forces on Centrifugal Pump Impellers," ASME Journal of Fluids Engineering, *110*, pp. 20-28 (1988).
7. Hergt, P. and Krieger, P., "Radial Forces in Centrifugal Pumps with Guide Vanes," Proc. Inst. Mech. Eng., *184* (Part 3N), pp. 101-107 (1969-70).
8. Jery, B., Acosta, A. J., Brennen, C. E. and Caughey, T. K., "Forces on Centrifugal Pump Impellers," *Proceedings of the Second International Pump Symposium*, Turbomachinery Laboratory, Texas A&M University, College Station, Texas (1985).

9. Ohashi, H., Sakurai, A., and Nishihama, J., "Influence of Impeller and Diffuser Geometries on Lateral Fluid Forces of Whirling Centrifugal Impeller," Fifth Workshop on Rotordynamic Instability Problems in High-Performance Turbomachinery, CP 3026, Texas A&M University, College Station, Texas (1988).
10. Stepanoff, A. J., *Centrifugal and Axial Flow Pumps*, New York, New York: John Wiley & Sons, pp. 116-123 (1957).
11. Hydraulic Institute Technical Specification No: TS001-C. Calculation of Radial Thrust for Volute Pump.
12. Biheller, H. J., "Radial Force on the Impeller of Centrifugal Pumps with Volute, Semivolute, and Fully Concentric Casings," ASME Journal of Engineering for Power, pp. 319-323 (July 1965).
13. Hydraulic Institute Technical Specification No: TS002-D. Calculation of Axial Thrust for Volute Pump.
14. Bolleter, U., Wyss, A., Welte, I., and Sturchler, R., "Measurements of Hydrodynamic Interaction Matrices of Boiler Feed Pump Impellers," ASME Paper No. 85-DET-148 (1985).
15. Ohashi, H. and Shoji, H., "Lateral Fluid Forces on a Whirling Centrifugal Impeller" (2nd Report: "Experiment in Vaneless Diffuser"), ASME Journal of Fluids Engineering, *109*, (2), pp.100-106 (1987).
16. Pottie, K., Wallays, G., Verhoeven, J., Sperry, R., Gielen, L., De Vis, D., Neumer, T. and Matros, M., "Active Magnetic Bearings used in BW/IP Centrifugal Pumps," Fourth International Symposium on Magnetic Bearings, Zurich, Switzerland (1994).
17. Guinzburg, A. and Buse, F. W., "Axial and Radial Forces on a Pump Impeller Obtained with a Magnetic-Bearing Force Measurement Rig," Fourth International Symposium on Magnetic Bearings, Zurich, Switzerland (1994).